An integrated study on the low-velocity impact response of fibre-reinforced laminated composite panels

Zheng He, Xuan Gu *, Xiaoyu Sun, Jianxin Teng, YingShu Pang

College of Aerospace and Civil Engineering, Harbin Engineering University, Harbin 150001 China

* guxuan@hrbeu.edu.cn

Abstract

This work is concerned with physical testing of carbon fibrous laminated composite panels with low velocity drop-weight impacts from flat and round nose impactors. Eight, sixteen, and twenty-four ply panels were considered. Non-destructive damage inspections of tested specimens were conducted to approximate impact-induced damage. Recorded data were correlated to load–time, load–deflection, and energy–time history plots to interpret impact induced damage. Data filtering techniques were also applied to the noisy data that unavoidably generate due to limitations of testing and logging systems. Built-in, statistical, and numerical filters effectively predicted load thresholds for eight and sixteen ply laminates. However, flat nose impact of twenty-four ply laminates produced clipped data that can only be de-noised involving oscillatory algorithms. Data filtering and extrapolation of such data have received rare attention in the literature that needs to be investigated. The present work demonstrated filtering and extrapolation of the clipped data using Fast Fourier Convolution algorithm to predict load thresholds. Selected results were compared to the damage zones identified with C-scan and acceptable agreements have been observed. Based on the results it is proposed that use of advanced data filtering and analysis methods to data collected by the available resources has effectively enhanced data interpretations without resorting to additional resources. The methodology could be useful for efficient and reliable data analysis and impact-induced damage prediction of similar cases' data.

Keywords

Carbon fibre; Polymeric composites; Mechanical testing; Data filtering.

1. Introduction

Widely used drop-weight impact testing and damage measuring procedures of laminated plates are documented in (ASTM: D7136). Impact damage resistance and damage tolerance of fibre reinforced laminated composites using different approaches to assess impact induced damage are reported in[1-2]. Effect of impactor shapes and geometries were investigated in[3-5]. The damage response on multilayer plates and stacking sequences is reported in[6-7]. Mainly utilised non-destructive techniques in aircraft industry consisting of: visual inspection, ultra-sonic C-scans and Eddy-current are reported in[8-9]. The techniques produce a planar indication of the type and extent of damage to detect certain kinds of damage distribution and progression without causing any major damage to the laminate that can be re-used or further tested. Main disadvantages and limitations of using the techniques are: whole structure has to be inspected, inspection process causes interruptions in normal operations and delays, and produces two-dimensional scan plots where multi-plane delaminations are projected on a single plane[10-12]. Hence, the techniques need to be supplemented with the data analysis for impact induced damage interpretations and analyses. Common difficulty in measuring

data, analysis, and damage detection is the contamination of noise due to vibration of impactor, target, rig, and other apparatus at different frequencies [13].

Impact generated data were filtered, threshold loads were predicted, compared and correlated to the relevant C-scan identified damage zones and were found within acceptable (±12%) deviations. The results proposed that use of advanced data filters can enhance interpretation of the data recorded with the available resources and make the investigation more efficient and reliable.

2. Experimental

Carbon fibre composites were developed by combining two or more engineering materials reinforced with strong material fibres to obtain a useful third material that exhibits better mechanical properties and economic values. Most of the composite materials are made by stacking several distinct layers of unidirectional lamina/ply made of the same constituent materials: matrix and fibres. The laminates used in this study were donated by industry, made of aerospace grade carbon fibre reinforced toughened epoxy infused Fibre dux 914C-833-40 embedded with satin weave fibre horn technique of every fifth ply. Stacking sequence code is [0/45/-45/90]*n*s for the symmetrical laminates where the subscript 's' stands for symmetric and '*n*' varies from 1, 2, and 3 for repetition of the lay-ups. In-plane dimensions of the laminates consist of plane dimensions of 150 mm × 120 mm. Panels have average variable thickness: 2.4 (±0.02), 4.8 (±0.023), and 7.2 (±0.026) mm respectively as shown in schematic view Fig. 1.

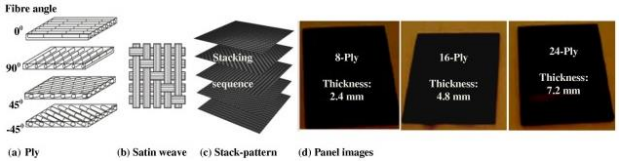

Fig. 1. Plies with fibre rotations, stain weave, stack, and laminated panels.

An outline of the investigation is depicted in flowchart Fig. 2. Physical tests were conducted of the panels shown in Fig. 1. Non-destructive examinations of the impacted specimens were performed. Impact produced data were analysed using built-in, statistical, numerical and fast Fourier filters. Data analysis assisted using filters to remove the low frequency impact response so that they could not dominate the high frequency signals.

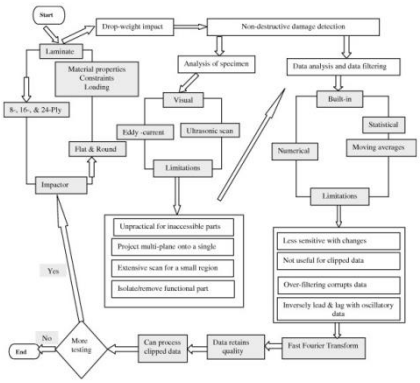

Fig. 2. Flowchart depicting stages of present work.

The tests were performed analogous to the actual impact event of real materials using an instrumented drop-weight testing system, INSTRON™ Pneumatic Dynatup System 9250HV (Products, 2011) shown in Fig. 3. The drop-weight machine represents situations such as accidentally falling of drop hammer, tool (box) during fabrication or maintenance, kitchen van etc.

A plane coordinate system is assumed to locate initial and final positions of the diameter of the damaged area. The damage length and width as shown in Fig. 4a radiating from the impact site at the centre is calculated by measuring distance with errors around 5% due to the ambiguous boundaries. The damaged area is assumed to map on ellipse/circles by adding or subtracting rectangular mesh elements/cells (width: 8 and length: 6 are indicated by double arrows) as shown in Fig. 4b. The

damaged area is then divided by the laminate area to obtain an approximate damage percentage. Dimensions of the panels are defined in Fig. 1.

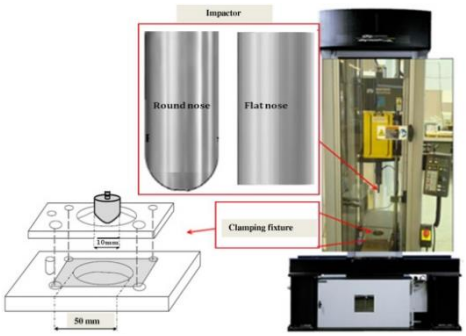

Fig. 3. INSTRON™ 9250 HV impact test machine.

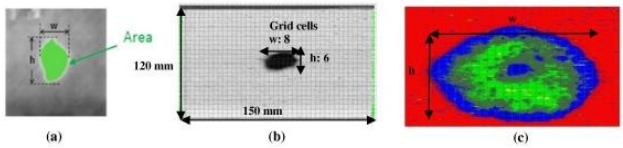

Fig. 4. Schematic of impact (a) damage area; (b and c) grid map of damage area.

Damaged areas detected by C-scan tests were approximated for 16-Ply panel of uniform scale as in Fig. 5a impacted at velocity: 1.7, 2, 2.2, 2.4, and 3.4 m/s by flat nose impactor. The figures show variations in damaged zones in the scanned images for five typical laminates subjected to increasing impact force levels. The approximated damaged area in each laminate corresponds to the impact loads that grew smoothly showing a relation between impact force and the damage size. In a relatively low loading case given inFig. 5a and b, no obvious damage can be observed visually near contact zone at the laminate surface by naked-eyes though it existed inside the laminate as detected by scan. Furthermore, for impact with slightly higher impact load, increased damage can be observed in Fig. 5d and e. This indicates a direct proportion between the loading cases and the macroscopic damages.

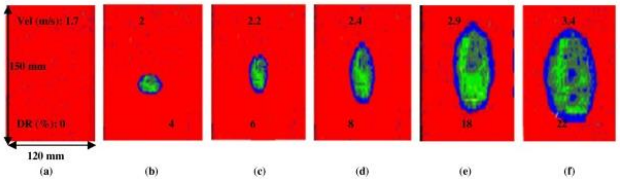

Fig. 5. C-scanned images of impact damaged are ratios (%).

To further explore validation of the FFT filtered and extrapolated results, the 24-Ply laminates impacted at velocity range 3.1–4 m/s were selected for comparison. Similar discussion applies to the results. The comparison of C-scan detected approximate areas of 24-Ply laminate impacted by flat nose impactor are shown in Fig. 6a–f damage area ratios (21%) that corresponding plot is shown in Fig. 7 against load of 24 kN compares well to filtered results in depicted load 22 kN. In-plane scales of all the panels are the same as shown inFig. 6a.

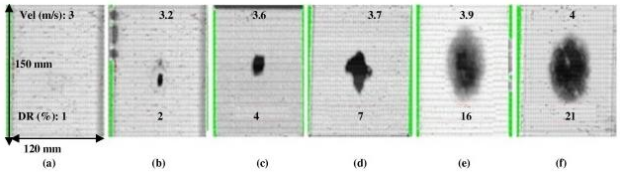

Fig. 6. C-scanned images of 24-Ply panels: velocity versus damage area ratio (DR: %).

To visualise the relationship, the history of the load and damage quantities approximated by C-scan images were put together to observe the correlation in plot. Corresponding best-fit plot of load versus damage area ratios up to (23%) is shown in Fig. 7. The linear regression relation shows peak load value up to 25 kN to the (22–23%) damage area. The roughly linear relation between the damage area and load drop of the pulse correlates well for characterising the load threshold where damage initiates.

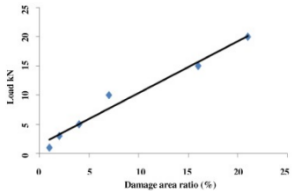

Fig. 7. Comparison of load versus C-scanned damaged area ratio (%).

However, non-destructive inspections are limited as shown in Fig. 2.

3. Results And Discussion

The first part of the curve is linear and represents the stiffness of the non-damaged laminate. The second part of the load–deflection curve shows a load drop as a clear change in stiffness, indicating damage initiation. Third and fourth parts are concerned with through-thick and perforation. The proposed oscillations and changes in load–deflection curve due to fibre breakage, matrix cracks, de-lamination, and ply failure in plots of impact generated data were utilised to correlate and interpret threshold load of the impacted panels Fig. 8. Energy–time history traces can also be used to correlate and predict strain and elastic energy levels during impact event.

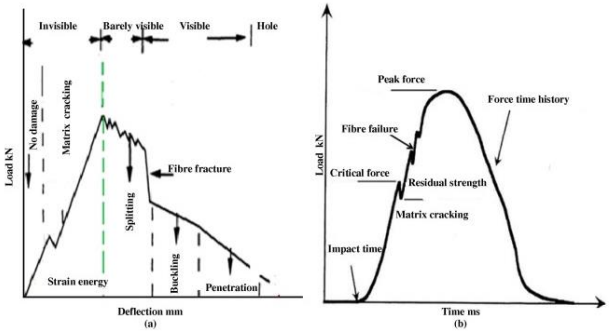

Fig. 8. Schematic of possible damage modes.

Drop-weight impact tests were conducted out on 8-Ply laminate using flat nose impactors at velocity: 2.2, 2.41 and 3.12 m/s. Data recorded from two impact tests at velocity 2.2 m/s were filtered and plotted in Fig. 9a. Curves show consistent behaviour and a load drop at around 7 kN that indicates failure. Built-in filtered data recorded from impacts at velocity 2.41 and 3.12 m/s are plotted in Fig. 9b. Comparison of the plot shows different levels of curves for different impact velocities. Load drops around 5.5 kN indicate failure due to severe cracking Fig. 8. This indicates that the data acquisition system and built-in filter can gather and filter data for this range of impact velocities and laminates.

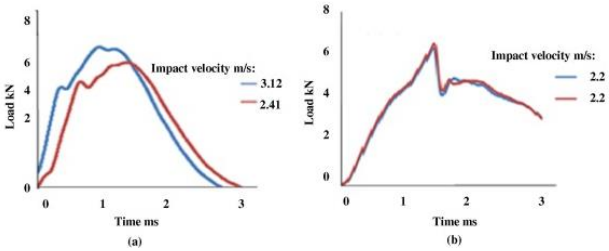

Fig. 9. Load–time history of 8-Ply laminate: (a) same, (b) different velocities.

Drop-weight impact tests were conducted on 8-Ply laminate using flat and round nose impactors at velocity: 2.2 and 2.8 m/s. Data were recorded for two tests and filtered. Data from impact at velocity 2.2 m/s are plotted in Fig. 10a. The curve representing data plot from flat nose impactor shows a load drop around 7 kN while round nose curve shows a load drop around 3.5 kN [14]. Similarly, data from two tests were recorded and filtered from impact at velocity 2.8 m/s and plotted in Fig. 10b.

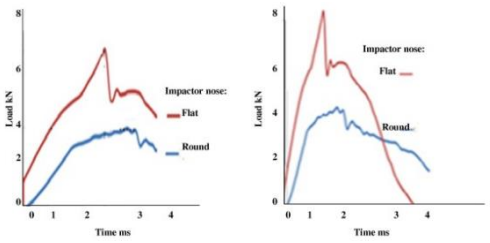

Fig. 10. Load–time response of 8-Ply panels under different impactor nose profiles.

Graphical comparisons of the test generated and filtered data were correlated to the irregularities in applied load to interpret useful information about how the material behaves during the impact process. Selected plot of deflection curves under flat nose impact of 8-Ply laminate at velocity 2.2 m/s trace in Fig. 11a were compared to curves in Fig. 11b [1]. Both the results show a severe load drop at around 7 kN that indicates ply level failure. This confirms that prediction of threshold load from interpretation of recorded and filtered data of the impact events are reliable and realistic.

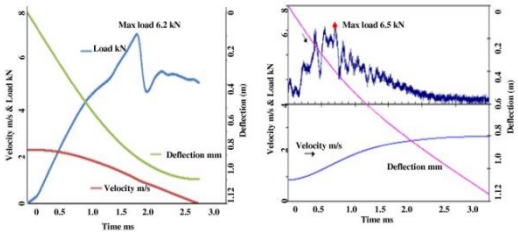

Fig. 11. Velocity–, load– and deflection–time history compared to data in [1].

Drop-weight impact tests were performed to investigate influence from the flat and round nose impacts of 8-Ply laminates of at velocity 1.6 m/s. The test generated data were recorded during the impact process and column-chart was plotted. No sudden/abrupt fluctuation of load drop can be seen from column-chart for both the impactor shapes. The comparison of load–deflection quantities created from the flat and round nose impactors is shown in Fig. 12. This confirms that impact-induced damage from round and flat nose impactors do not show much difference for the impact velocity range up to 1.6 m/s using built-in filters.

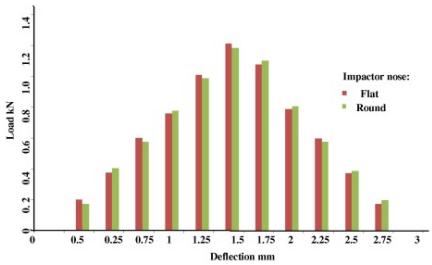

Fig. 12. Load–deflection response of 8-Ply impacted at velocity 1.6 m/s.

Drop-weight impact tests were conducted on 16-Ply laminate using flat and round nose impactors at velocity: 3.12 m/s. Recorded data were filtered and are plotted inFig. 13a and b that depicts closed loops. The elastic impact and rebound curve for round nose shows consistent behaviour to some extent, the load drops around 11 kN that indicates failure. However, filtered data gathered from flat nose impact show slightly inconsistent behaviour. Instead of load drop it shows negligible constant loading line like plastic behaviour after load range 14 kN.

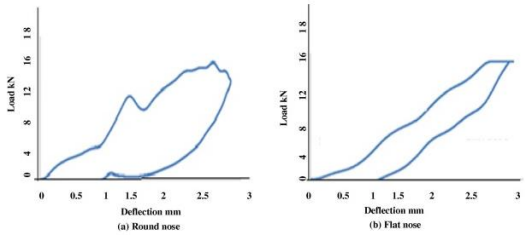

Fig. 13. Load–deflection response of 16-Ply panel with round and flat nose impacts.

Drop-weight tests were performed on 24-Ply laminates impacted by flat and round nose impactors at impact velocity 3.74 m/s. Data filtered and recorded by built-in data acquisition system were plotted. Fig. 14 shows load drop after 13 kN in curve representing round nose impact while inconsistent tendencies after 17 kN can be seen in curve that represents flat nose impact.

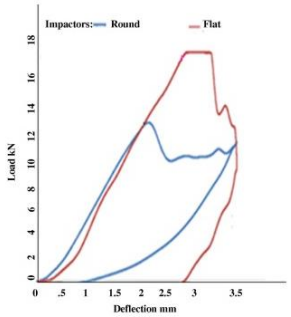

Fig. 14. Load–deflection of 24-Ply laminate impacted versus impactor nose profiles.

Comparisons of the test generated data for 24-Ply laminate impacted by flat and round nose impactors at velocity 3.74 m/s are plotted in Fig. 15a and b. Curves relating to flat nose impact for velocity and deflection parameter also show consistent behaviour.

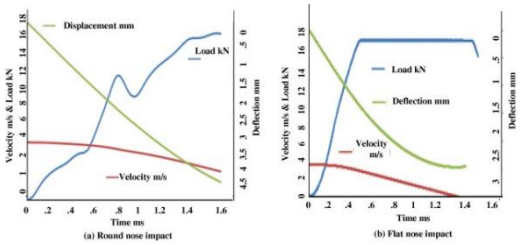

Fig. 15. Velocity–, load–, and deflection– time history of 24-Ply laminate.

Application of the algorithm is illustrated for the flat nose impact of 24-Ply panels impacted at velocity 3.74 m/s in plots of Fig. 16 below.The energy–time history traces show influence of impactor nose profiles in respect of impact-induced damage. It can be seen that despite the same velocity both the impactors attain slightly different impact energy levels Fig. 16.

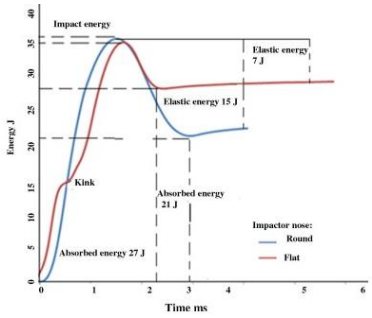

Fig. 16. Energy history of 24-Ply laminate impacted at velocity 3.74 m/s.

To further confirm the inconsistent behaviour, data from round and flat nose impact tests of 16- and 24-Ply laminates were recorded, filtered, and plotted in Fig. 17a and b. Consistent and expected behaviour was observed in velocity, deflection, and energy history time plots. Load–time histories were found to be as expected. However, the elastic impact curves for flat nose impactor of 24-Ply laminates show inconsistent behaviour to some extent and load curves show plastic type behaviour near 17 kN. The inconsistent behaviour in load–time plot before reaching 80 kN of machine's specification cut-off of frequency indicates limitations of data logging and impact system. This could be attributed to the flat nose type of impactor and relatively thick laminates consisting of 24-Ply. The data of Fig. 17b were filtered utilising numerical algorithms but not much improvement was achieved.

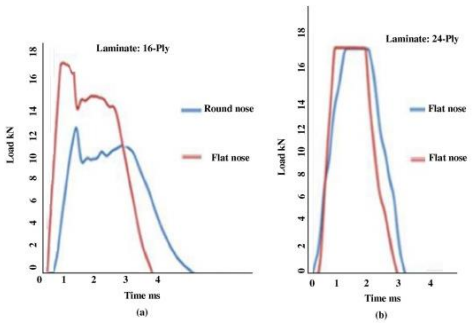

Fig. 17. Load–time traces of 16-, 24-Ply laminates versus impactor nose profiles.

Roots of unity (w) and periodic symmetry facilitate to compute the root once and split it into odd and even using basic relations enπi=cosnπ+isinnπ=(-1)n shown in Fig. 18.

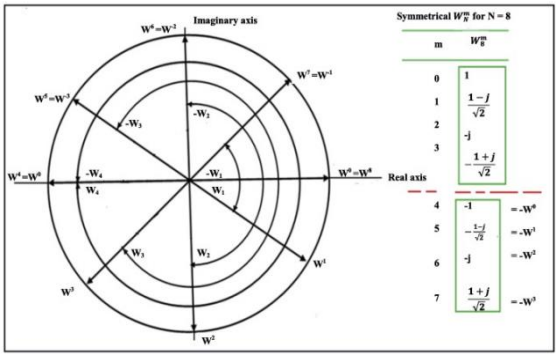

Fig. 18. Computational symmetry & data split in even and odd sub-sequences.

The WN (n th root of unity) values are the coefficients of the FFT and are often referred to as twiddle factors (complex exponential values). Because of its shape the basic computational unit of the FFT is called a butterfly (because of its crisscross appearance), simplified by factoring out a term W_N^{nk} from the lower branch as illustrated in Fig. 19. The factor that remains is $W_N^{N/2} = -1$. Each of the building blocks has the following structure:

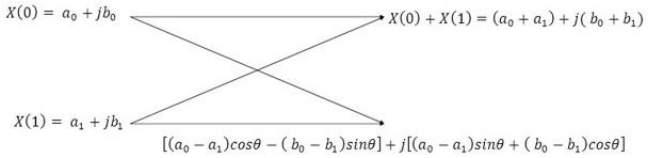

Fig. 19. Schematic of possible values at first and second stages.

Comparison of the curves in Fig. 20a and b shows that filtering process had raised the peak load quantities from 16 to 18 kN. Moreover, load drops occur at peak load (threshold) indicating matrix cracking failure. No significant straight line portions of curves depicting clipped data can be seen. The results suggest that the threshold could be predicted without resorting to advanced filtering algorithms for these types of impacts.

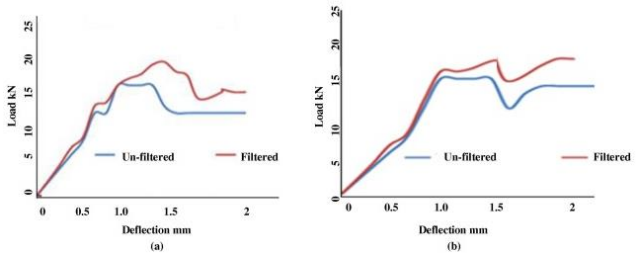

Fig. 20. Filtered load–deflection plot of 16-Ply versus flat and round nose impact.

Another set of data obtained for 16-Ply panels impacted at velocities 3.8 m/s were filtered using fast Fourier algorithms (convolution based) and extrapolated to correlate to predict load threshold. It can be seen from the curves that drops occur approximately around 15 kN around 1.5 mm deflection for round nose impactor and load drop occurs at 20 kN under flat nose impact at 2.5 mm deflection in

Fig. 21a. The data filtering algorithm successfully predicted threshold load as expected for the relatively thin panel.Separate tests were conducted of relatively thick 24-Ply panels impacted at 4 m/s velocity with flat nose impactor. Load–deflection curves for un-filtered data show straight line of clipped data after around 18 kN as shown in Fig. 21b.

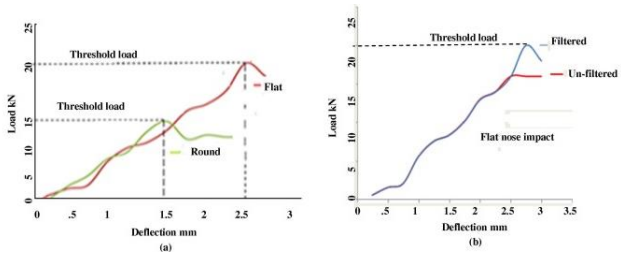

Fig. 21. Filtered load–deflection plot of 16-Ply under flat and round nose impact.

The same filtering and extrapolating process was applied to the data obtained from impacts of relatively thick 24-Ply panels at 3.74 and 4.2 m/s velocities impacted with flat nose impactors. Plots of the filtered and un-filtered data are shown in Fig. 22. It can be seen that the load level increased from19 to 23 kN with velocity 3.74 m/s where expected load drop occurred Fig. 22a. The plot of impact with 4.2 m/s velocity shows increase in the load level from 20 to 24 kN and where load drop occurred (peak load as the threshold load) Fig. 22b.

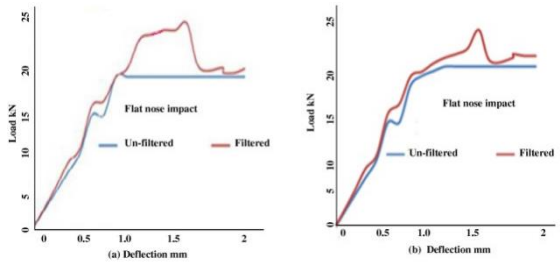

Fig. 22. Load–deflection of 24-Ply panels impacted with flat nose impactors.

4. Conclution

Based on the results it is proposed that use of advanced data filters can enhance data interpretation and make the investigation more efficient and reliable. The proposed methodology could be useful for efficient and reliable data analysis and impact-induced damage prediction of similar case data.

Acknowledgements

This work is supported by the National Natural Science Foundation of China(No. 11602066) and the National Science Foundation of Heilongjiang Province of China (QC2015058 and 42400621-1-15047), the Fundamental Research Funds for the Central Universities.

References

[1] James RA. Impact damage resistance and damage tolerance of fibre reinforced laminated composites [Ph.D. thesis]. United Kingdom: University of Bolton; 2006.
[2] R. Hosseinzadeh, M.M. Shokireh, L. Lessard Damage behaviour of fibre reinforced composite plates subjected to drop weight impacts Compos Sci Technol, 66 (2005), pp. 61–68
[3] T. Mitrevski, I.H. Marshall, R.S. Thomson, R. Jones Low-velocity impacts on preloaded GFRP laminates with various impactor shapes Compos Struct, 76 (2006), pp. 209–217
[4] S. Kumar, B. Nageswara, B. Pradhan Effect of impactor parameters and laminate characteristics on impact response and damage in curved composite laminates J Reinforced Plastics Compos, 26 (13) (2007), pp. 1273–1290
[5] S. Ercan, L. Benjamin, D. Feridun Drop-weight impact response of hybrid composites impacted by impactor of various geometries Mater Des, 52 (2013), pp. 67–77

[6] Y. Deng, W. Zhang, Z. Cao Experimental investigation on the ballistic resistance of monolithic and multi-layered plates against hemispherical-nosed projectiles impact Mater Des, 41 (2012), pp. 266–281
[7] C.S. Lopes Low-velocity impact damage on dispersed stacking sequence laminates. Part I. Experiments Compos Sci Technol, 69 (7–8) (2009), pp. 926–936
[8] U. Farooq, P. Peter Myler Finite element simulation of buckling-induced failure of carbon fibre-reinforced laminated composite panels embedded with damage zones Acta Astronaut, 115 (2015), pp. 314–329
[9] Y.O. Kas, C. Kaynak Ultrasonic C-scan and microscopic evaluation of resin transfer moulded epoxy composite plates Polym Testing, 24 (2004), pp. 114–120
[10] Y.O. Kas, C. Kaynak Ultrasonic C-scan and microscopic evaluation of resin transfer moulded epoxy composite plates Polym Testing, 24 (2004), pp. 114–120
[11] U. Polimeno, M. Michele, D.P. Almond, S.L. Angioni Detecting low velocity impact damage in composite plate using nonlinear acoustic/ultrasound methods Appl Compos Mater, 17 (2010), pp. 481–488
[12] G. Mook, R. Lange, O. Koeser Non-destructive characterisation of carbon-fibre-reinforced plastics by means of Eddy-currents Compos Sci Technol, 61 (2001), pp. 865–873
[13] C.N. Della, D. Shu Vibration of delaminated composite laminates: a review Appl Mech Rev, 60 (2007), pp. 1–2
[14] U. Farooq, P. Myler Efficient computational modelling of carbon fibre reinforced laminated composite panels subjected to low velocity drop-weight impact Mater Des, 54 (2014), pp. 43–56